

Analysis of Different Designed Landing Gears for a Light Aircraft

Essam A. Al-Bahkali

Abstract—The design of a landing gear is one of the fundamental aspects of aircraft design. The need for a light weight, high strength, and stiffness characteristics coupled with techno economic feasibility are a key to the acceptability of any landing gear construction. In this paper, an approach for analyzing two different designed landing gears for an unmanned aircraft vehicle (UAV) using advanced CAE techniques will be applied. Different landing conditions have been considered for both models. The maximum principle stresses for each model along with the factor of safety are calculated for every loading condition. A conclusion is drawing about better geometry.

Keywords—Landing Gear, Model, Finite Element Analysis, Aircraft.

I. INTRODUCTION

THE landing gear is one of the most critical components of an aircraft, which capable of reaching the largest local loads on the airplane. It is the structure that carries an aircraft during taxi, take-off, and landing. Moreover, it is a primary source of shock attenuation at landing. It controls the rate of compression, extension, and prevents damage to the aircraft. Therefore, greatest care must be taken into consideration through designing the main landing gear.

To construct a landing gear it is essential to identify the type, geometry, and weight of the aircraft. Young [1] talked about landing gear basic requirements. He also made a review for historic and current equipment designs. He finally concluded by pointing to possible future developments to enhance functional efficiency. Sadraey [2] consider ten important parameters in designing any landing gear. Some of these parameters are: the height, the wheel base, the distance between main landing gear and aircraft center of gravity, strut diameter, tire sizing, and the load on each strut. Goyal [3] published a paper relating to the design of a light landing gear using finite element method. He showed that the most significant feature of the analysis was the thickness with buckling, stress and different failure criteria. He also showed that the material used for making the main landing gear should have high elastic strain energy storage capacity. The desired characteristics of a main landing gear are high strength, lightweight, medium stiffness, and high elastic strain energy storage capacity.

In this paper, two different configuration landing gears for a small UAV will be analyzed using finite element (FE) method. The analysis is started by building the models to study and

compare the distribution of developed stress and strain fields. Different modeling parameters will be studied to come up with the proper element type, loadings, constraints, materials and model behavior.

In the development phase, a rigorous non-linear stress [4] and deflection analysis are carried out. A true assessment of the critical regions is made so as to predict the behavior of the landing gear at extreme landing conditions. A margin of safety is also determined for different loading conditions. Finally, a conclusion is done.

II. FINITE ELEMENT MODELING

A. Geometric Models

Two different models are considered. These models are a landing gear with a straight ends (Model 1), which can be seen in Fig. 1, and a landing gear with bend ends (Model 2), which can be seen in Fig. 2. The geometries of both landing gear models are shown below.

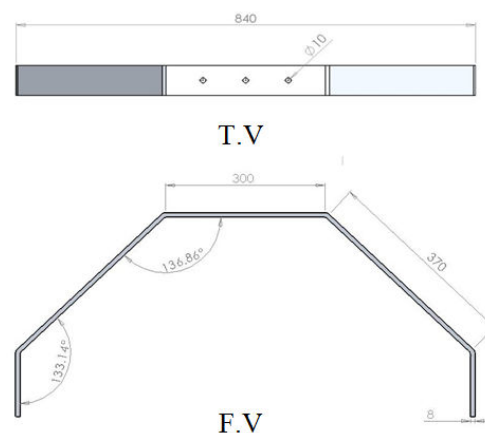


Fig. 1 Geometry details of Model 1 (All dimensions in mm)

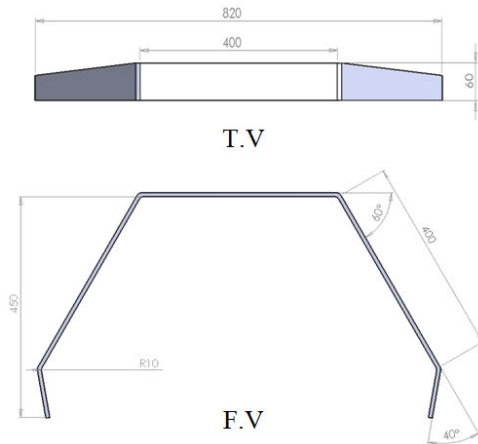


Fig. 2 Geometry details of Model 2 (All dimensions in mm)

B. General Assumptions

The following assumptions are considered: The landing gears are modeled using three-dimensional FE analysis and the maximum weight of the UAV is 80kg. The friction force developed at the tire, the tangential force developed by the inertia force, the moment developed by the vertical load times the distance from center of gravity to the landing gear, the stiffness of the tire are all neglected.

C. Landing Conditions

It is assumed that the UAV is landed with a vertical speed between 2 and 8m/s. In addition, the UAV is landed at normal glide angle between 3 to 10 degrees. Where the glide angle is the angle measured from the ground.

Based on the given speeds, the impact force can be calculated using the impulse momentum equation:

$$F\Delta t = mV_f \quad (1)$$

where F is the impact force, Δt is the impact time, m is UAV weight, and V_f is the vertical velocity at the impact.

Assuming that the time of impact is about $\Delta t = 0.5$ second, thus the impact load at landing for the range of speed given above are shown in Table I.

TABLE I
IMPACT LOADS CORRESPONDING TO DIFFERENT LANDING SPEEDS

Case	V_f (m/s)	F (N)
1	2	320
2	2.5	400
3	3	480
4	3.5	560
5	4	640
6	4.5	720
7	5	800
8	5.5	880
9	6	960
10	6.5	1040
11	7	1120
12	7.5	1200
13	8	1280

D. Boundary Conditions

The mechanical boundary conditions associated with each finite element model can be shown in Fig. 3 and are summarized as the following:

On the top surface of the landing gear, a clamped boundary conditions are imposed between landing gear and fuselage (orange points). Thus, the displacements become:

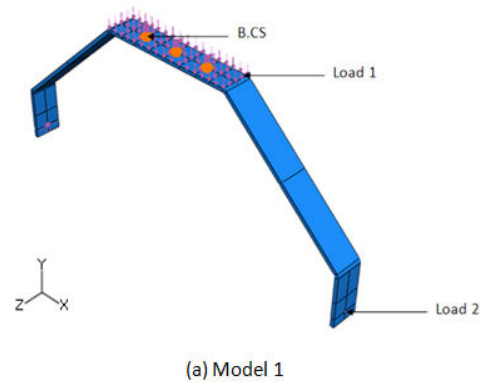
$$u_x = u_y = u_z = 0 \quad (2)$$

The UAV weight (Load 1) is applied in the negative y-direction at the top surface of the landing gear.

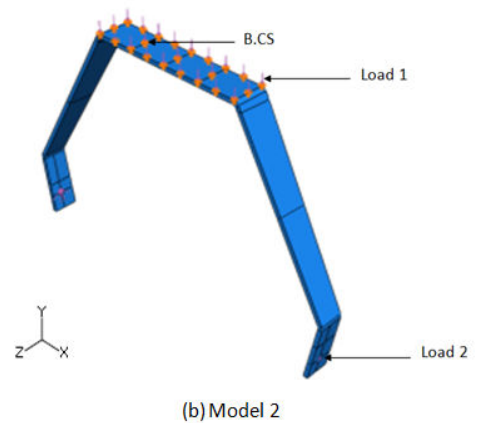
$$F_y = -mg \quad (3)$$

The impact load at the bottom of the landing gear is applied along the positive y-direction.

$$\text{Impact load} = F \quad (4)$$



(a) Model 1



(b) Model 2

Fig. 3 Boundary conditions for (a) Model 1 and (b) Model 2

E. Material Used in Both Models

The material that is used in the analysis is Aluminum Alloy 7075-T6 [5]. It is the most common material used for landing gear (see Table II).

TABLE II
MECHANICAL PROPERTIES OF AL 7075-T6 ALUMINUM ALLOYS

Mechanical Properties	Al 7075-T6
Hardness, Vickers (VH)	175
Tensile Yield Strength (MPa)	503
Ultimate Tensile Strength (MPa)	572
Elongation at Break (%)	11

F. Finite Element Meshing

The finite element computation is carried out using ABAQUS software [6]. The finite-element meshes of these models are generated using eight-node-linear brick reduced integration elements (C3D8R). Fig. 4 shows the finite element meshes for both models. The numbers of elements for the both models that used in the current study, after several refined meshes to insure the conversion of the FE results, are given in Table III.

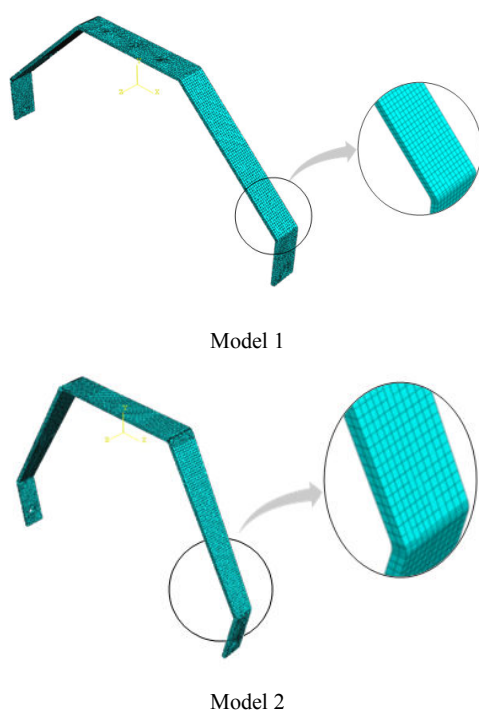


Fig. 4 Finite Element Meshing for both Model 1 and 2

TABLE III NUMBER OF ELEMENT USED IN THE TWO MODELS		
Model	Model 1	Model 2
No. of Element	6700	6894

III. RESULTS

The thirteen cases described in Table I have been used for both models. Samples of the results achieved from these finite element runs are shown in Fig. 5 for model 1 and Fig. 6 for model 2.

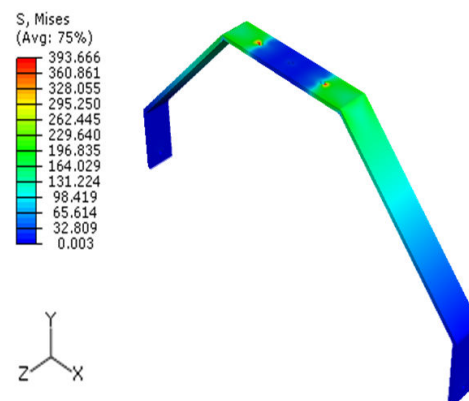


Fig. 5 Von Mises Stress contour for Model 1 using loading condition case 12

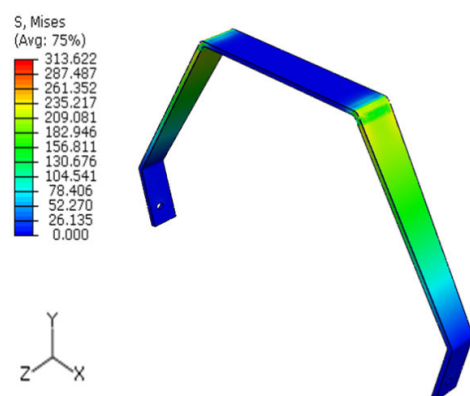


Fig. 6 Von Mises Stress contour for Model 2 using loading condition case 12

Table IV shows the summary of the two models subjected to all possible landing conditions discussed in Table I. It displays the values of the maximum stresses developed in the model according to the respective loading conditions along with the calculated factor of safety as compared to the yield strength of the material.

For Model 1, it is found that the factor of safety was always above one, ranging from 5.17 to 1.2 in going to the most sever landing conditions (case 12). For Model 2, the factor of safety was always above one, ranging from 6.01 to 1.5 in going to the most sever landing conditions (case 12).

TABLE IV
STRESS AND FACTOR OF SAFETY FOR MODEL 1 AND MODEL 2

Case	V (m/s)	F (N)	Model 1		Model 2	
			Maximum Stress	Factor of Safety	Maximum Stress	Factor of Safety
1	2	320	97.21	5.17	83.63	6.01
2	2.5	400	124.17	4.05	104.54	4.81
3	3	480	151.12	3.33	125.45	4.01
4	3.5	560	178.07	2.83	146.36	3.44
5	4	640	205.02	2.45	167.27	3.01
6	4.5	720	231.97	2.17	188.17	2.67
7	5	800	258.92	1.94	209.08	2.41
8	5.5	880	285.87	1.76	230.00	2.19
9	6	960	312.82	1.61	250.90	2.01
10	6.5	1040	339.77	1.48	271.81	1.85
11	7	1120	363.72	1.38	292.71	1.72
12	7.5	1200	393.67	1.28	313.62	1.60
13	8	1280	420.62	1.20	334.53	1.50

Fig. 7 represents the variation of Von Mises stresses with landing velocity for both models 1 and 2. It showed that Model 2 is always less in stresses for any landing conditions. Fig. 8 represents the variation of factor of safety with landing velocity for both models. It is obvious from the fact that the factor of safety was in all cases above one that this material is a suitable material to be used for manufacturing the landing gear. In addition, Model 2 is always safest than Model 1 for any landing conditions.

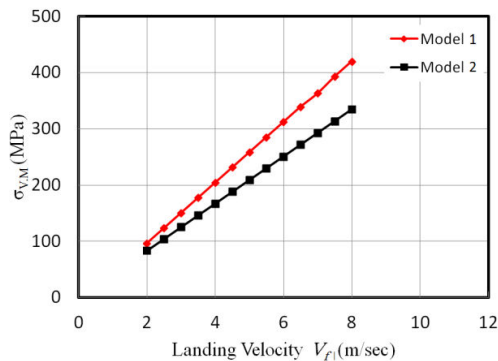


Fig. 7 Von Mises Stresses versus landing velocity V_f for both Models

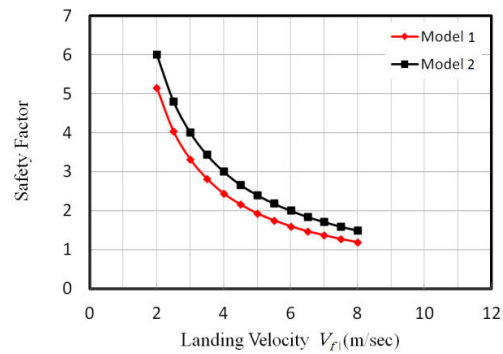


Fig. 8 Safety Factor versus landing velocity V_f for both Models

IV. CONCLUSION

Two different landing gears configuration have been analyzed and modeled using a commercial finite element code (ABAQUS). Different landing conditions have been considered for both models (thirteen different loading conditions that were calculated from different landing speeds).

For AA7075-T6 used for both models, the factor of safety rendered was above one for all loading cases. This shows that this material is a suitable material to manufacture the landing gear. In addition, model 2 yields higher factor of safety for each case and consequently leads to more conservative design.

REFERENCES

- [1] D.W. Young, "Aircraft Landing Gears—Past Present and Future", *Proceeding of IME*, Vol. 200, No. D2, pp 75-92, 1986.
- [2] M. H. Sadraey, "Aircraft Design: A Systems Engineering Approach", Wiley, 2012.
- [3] A. Goyal, "Light Aircraft Main Landing Gear Design and Development", *International ANSYS Conference Proceedings*, 2000.
- [4] R.H. Mallett and P.V. Marcal, "Finite Element Analysis of Non-linear structures", First Division, Vol. 94, No. ST9, pp. 2081 – 2105, 1968.
- [5] Metals Handbook, Properties and Selection: Nonferrous Alloys and Special-Purpose Materials, ASM International, Vol.2, 10th edition. 1990.
- [6] ABAQUS, User's Manual, Version 6.9, 2010.